

Identification of a compound series by High Throughput Screening capable of
reversing the antiviral effect of Ribavirin in tissue culture

by

Jonathan M. Gallion

A PROJECT

submitted to

Oregon State University

University Honors College

in partial fulfillment of
the requirements for the
degree of

Honors Baccalaureate of Science in Biochemistry/Biophysics (Honors Scholar)
And
Honors Baccalaureate of Science in Microbiology (Honors Scholar)

Presented June 14, 2012
Commencement June 2012

AN ABSTRACT OF THE THESIS OF

Jonathan M. Gallion for the degree of Honors Baccalaureate of Science in Biochemistry/Biophysics and Honors Baccalaureate of Science in Microbiology presented on June 14, 2012 Title: Identification of a compound series by High Throughput Screening capable of reversing the antiviral effect of Ribavirin in tissue culture.

Abstract Approved:

Theo Dreher

A compound series capable of reversing the antiviral effect of Ribavirin (RBV) against H1N1 was identified from a high throughput screen designed to discover compounds capable of increasing the fidelity of the RNA-dependent RNA polymerase (RDRP) in ribovirus quasispecies. Two lead compounds, RIC-1 (EC50 of 78.4 nM) and RIC-2 (EC50 of 217 nM), returned viral growth to control levels by completely inhibiting the antiviral activity of RBV. Both compounds demonstrated a loss of activity when incubated at 37°C in media only, losing functionality within 3 hours. Incubation of RIC-1 or RIC-2 with cells for only 2.5 minutes, however, was able to maintain viral growth by inhibiting RBV for the full 72 hour growth period. Subsequent testing showed the RIC series was not effective against a second mutagen, 5-fluorouracil, and RIC-2 did not prevent or slow the development of antiviral resistance when viral populations were grown in the presence of Zanamivir. Furthermore, RIC-1 was ineffective in alleviating inhibition of the inosine 5'-monophosphate dehydrogenase (IMPDH) pathway by the inhibitor mycophenolic acid (MPA). Anti-RBV activity was relieved by increasing the concentration of RBV, suggesting the RIC series acts to competitively inhibit RBV. The mechanism of action associated with the RIC compound series is still unclear; however, it appears to act independent of the intended function of RDRP fidelity modification.

Key Words: Ribavirin (RBV), RDRP Fidelity, Influenza H1N1, Equilibrative Nucleoside Transporter (ENT-1), inosine monophosphate dehydrogenase (IMPDH)
Corresponding e-mail address: JGallion@sig.com

©Copyrighted by Jonathan M. Gallion
June 14 2012
All Rights Reserved

Identification of a compound series by High Throughput Screening capable of
reversing the antiviral effect of Ribavirin in tissue culture

by

Jonathan M. Gallion

A PROJECT

submitted to

Oregon State University

University Honors College

in partial fulfillment of
the requirements for the
degree of

Honors Baccalaureate of Science in Biochemistry/Biophysics (Honors Scholar)

And

Honors Baccalaureate of Science in Microbiology (Honors Scholar)

Presented June 14, 2012
Commencement June 2012

Honors Baccalaureate of Science in Biochemistry/Biophysics and Microbiology
project of Jonathan M. Gallion

APPROVED:

Mentor, representing SIGA Technologies Inc

Mentor, representing Microbiology

Committee Member, representing Microbiology

Chair, Department of Biochemistry/Biochemistry

Chair, Department of Microbiology

Dean, University Honors College

I understand that my project will become part of the permanent collection of Oregon State University, University Honors College. My signature below authorizes release of my project to any reader upon request.

Jonathan M. Gallion, Author

Acknowledgement

I would like to express a deep gratitude for SIGA Technologies and the people who work there. All research contained within this document was fully funded and supported by SIGA. This financial support continued to be provided even after my research was deemed to have no financial merit for the company. Furthermore, in addition to a personal salary I was allowed freedom and independence in all areas of the experimental process.

I would like to specifically thank Dr. Robert Allen, Dr. Robert Jordan, and Keith McKinley. The contributions given by Keith, RJ, and Robbie were essential to the progression of my research and the completion of this honors thesis. I am very thankful to have had the privilege to work with them. I would also like to thank Daniela Kropf for her time in creating a method and processing my samples on the Mass Spec. Furthermore, I was continually grateful to work with all the SIGA staff, as they provided a very enjoyable and productive working environment.

Finally I would like to offer my sincere thanks to my mentor at OSU Dr. Theo Dreher and my committee member Dr. Bruce Geller. Dr. Dreher was more than generous with his time, guidance and patience. His contributions to the writing process and my thesis as a whole were tremendously appreciated. Dr. Geller further contributed his time to my thesis, even at a short notice, of which I am very thankful.

TABLE OF CONTENTS

	<u>Page</u>
INTRODUCTION.....	1
METHODS.....	3
Cell Lines and Materials.....	5
Influenza Virus Infection.....	5
Primary High Throughput Screening	6
Secondary Screening	7
Tertiary Screen Assay Development.....	7
Antagonism Screening.....	8
Emergent Mutation Assay.....	9
Pre-incubation for chemical interaction between RIC-1 series and Ribavirin.....	10
Pre-incubation of RIC-1 and RIC-2 to measure rate of association.....	11
Ribavirin Uptake.....	12
Interaction of RIC series with the inhibition of the IMPDH pathway.....	13
RESULTS.....	14
High-Throughput Screening.....	14
RBV specificity testing using multiple nucleoside analogs.....	16
Emergent Mutation Assay.....	19
Preincubation to measure for a direct chemical inactivation of RBV.....	23
Rate of Association between RIC-1 and its Target Site.....	26
Cellular Uptake of RBV.....	28
RIC involvement with the IMPDH Pathway.....	30
DISCUSSION.....	32
REFERENCES.....	45

LIST OF FIGURES

Figure	Page
1. Ability of Lead compounds to return Influenza growth after treatment with 45 uM RBV.	15
2. Possible sites of interaction between the RIC compound series and RBV.....	16
3. Inhibitory effect of Ribavirin and 5-Fluorouracil on Influenza.....	17
4. Comparison of RIC-2's ability to relieve viral inhibition resulting from treatment with either RBV or 5FU.....	18
5. Cyclic serial passage treatment plan for selection of Zanamivir resistance in Influenza.....	20
6. Histogram showing effect of RIC-2 on the distribution of viral growth after serial passage in the presence Zanamivir.....	22
7. Effect of Preincubation on the RIC-1/RBV interaction.....	24
8. Effect of short incubation times on efficacy of RIC-1 and RIC-2 in inhibiting 45uM RBV.....	26
9. Cellular uptake of RBV by ENT-1 in the presence of RIC-1.....	29
10. Effect of RIC on IMPDH inhibition by Mycophenolic Acid (MPA).....	31
11. Efficacy of RIC-1 and RIC-2 against increasing RBV concentrations.....	40

Identification of a compound series by High Throughput Screening capable of reversing the antiviral effect of Ribavirin in tissue culture

Introduction

Many RNA viruses represent a severe health risk through chronic infections and sporadic epidemics [1]. Their rapid mutation rate complicates the treatment and prevention of diseases such as Human Immunodeficiency Virus (HIV), Hepatitis C, and Influenza [2-4]. Viral populations exist as a collection of genetically related mutants undergoing rapid adaptive evolution [5]. An infected individual can harbor multiple genotypically unique but related mutants of the same species, each capable of continued adaptive changes, making the treatment and management of an infection difficult [6]. The mutation rate of a viral population is dictated by the fidelity, or error rate, of the polymerase enzyme used. The RNA-dependent RNA polymerase of riboviruses operates with a characteristically low fidelity for the RNA strand and has an error rate of 10^{-3} to 10^{-5} mutations per nucleotide per replication event. This represents several orders of magnitude greater than the replication error rate of organisms with a DNA genome and results in rapidly evolving viral populations [7,8,9]. Given the large population size of a typical viral infection, it is possible that a population is at any time composed of mutants expressing every point mutation possible as well as many double mutations [7].

Quasispecies theory, originally used to describe population dynamics in the “precellular RNA world”, has been experimentally validated to further describe the population dynamics of RNA viruses [7,10,11,12]. The rapid rate of evolution coupled to a near

infinite population size creates a cloud of genetically distinct mutants, each contributing to the characteristics of the viral phenotype [14]. To varying extents for specific viruses, the standing genetic diversity of the genome population is curtailed by a selective loss of variants due to competitive disadvantages relative to the wild type. These specific variants would be lost from the population further strengthening the population as a whole.

Alterations in the overall structure and composition of the variants composing the population can drastically alter the pathogenesis of the virus [15,16,17]. While previous work on RNA viruses has focused on the replicative fitness of viral clones, fitness in a viral quasispecies is primarily dependent on the mutation and adaptation rate of the population as a whole rather than an individual mutant's replicative ability [1]. There is however an upper limit to the number of mutations per replication, known as the error threshold [1]. A polymerase that operates past this threshold causes a buildup of deleterious mutations in the resulting progeny, inducing an “error catastrophe” and lethal mutagenesis of the population [1]. RNA viruses have evolved with an optimized mutation rate thereby maximizing the diversity of the resulting viral population without crossing this threshold [18,19]. By operating just under the error threshold the population as a whole can exist in many different environments, which would have otherwise been outside the range of the original “master” virion.

Recent research has focused on using lethal mutagenesis as a natural form of antiviral defense and can be used as a viable therapeutic option in some viral infections [20,21]. Compounds which decrease the fidelity of the RDRP would push viral populations past

the error threshold resulting in the buildup of deleterious mutations. Of the compounds being tested, nucleoside analogs have shown the most promise. Ribavirin is a nucleoside analog with broad anti-viral activity, and is currently used therapeutically against respiratory syncytial virus (RSV) and HCV as well as demonstrating lethal mutagenesis in Hantaan and Polio viruses [22,23,24].

An alternate therapeutic option is paradoxically presented by increasing the fidelity of the RDRP. By limiting the mutation rate of viral quasispecies the maintained genotypic homogeneity results in a less fit, more treatable infection [1]. In dynamic environments a high mutation rate represents an evolutionary advantage and is advantageous to viral growth. While each variant may be less fit than the original genotype, the population has the ability to quickly adapt to an environmental pressure, such as an immune response. A viral population lacking this flexibility to adapt would not be able to mutate in response to a selective pressure and would therefore be more vulnerable to antiviral treatments. This theory has been effectively shown by two groups working on the polio virus [25,26]. A mutant with an altered polymerase resulting in a higher fidelity replication was less virulent and less capable of infection when compared to the wild type [27].

Using High Through-put Screening of a compound library, SIGA Technologies developed a screen to identify compounds capable of increasing the fidelity of an RNA virus's RDRP. Using Influenza H1N1 as a model virus, the screen uses ribavirin to artificially push Influenza past the error threshold resulting in an error catastrophe and inhibition of viral growth. Co-treatment with compounds that increase polymerase fidelity would inhibit the mutagenic effect of RBV saving the population from the error catastrophe and

resulting in a normal viral infection. A “hit” is any compound which reverses the anti-viral effects of RBV.

Due to the nature of this screen, positive hits may be compounds that simply act antagonistically to RBV thereby negating its mutagenic effects in a manner independent from the RDRP. Current research is unclear on RBV's mechanism of action in Influenza, although there are many proposed possibilities [28,29,30,31]. Firstly, RBV may act on the viral polymerase either as a viral mutagen decreasing polymerase fidelity [32,33,34] or by termination of chain elongation through incorporation of RBV triphosphate by the RDRP [35,36,37]. Alternatively ribavirin may inhibit activity of inosine monophosphate dehydrogenase (IMPDH) the host enzyme that catalyzes de novo synthesis of GTP [38,39,40]. Inhibition of IMPDH would result in a reduction of purine nucleotide pools necessary for viral replication. Due to the uncertainty in RBV's MOA, a compound showing promise in reversing the action of RBV may be acting in one of many ways to inhibit RBV, requiring the necessity of subsequent testing.

A compound which increases RDRP polymerase fidelity would limit a virus's ability to quickly mutate around the selective pressures of antiviral treatments and immune responses. Limiting the mutation rate of a quasispecies population would severely inhibit their ability to rapidly gain resistance to current antiviral treatments and leave them more vulnerable to therapeutic options. If used concurrently with antivirals a compound that increases RDRP fidelity might not only control acquired resistance but also limit the development of emergent infections possibly leading to eradication.

Methods

Cell Lines and Materials

Except where specified all experiments were conducted using Madin-Darby Canine Kidney (MDCK) cells. These cells were maintained in Eagle's Modified Essential Medium (EMEM) purchased from ATCC (catalog # 30-2003) supplemented with 10% fetal bovine serum (Invitrogen Catalog #10082-147), and 100 U of penicillin-streptomycin (penstrep)/ml (Invitrogen Catalog #15140-163). Cells beyond passage number 25 were not used experimentally. MDCK cells were seeded in serum free MDCK-ULTRA media supplemented with 100 U penstrep for each experiment. Fetal bovine serum was excluded as it interferes with glycosidic hydrolase activity of the influenza viral protein neuraminidase which is necessary for cellular entry. All cells were maintained at 37°C with 5% CO₂.

Zanamivir (Catalog #M-1826) was purchased from Moravek. The chemical 2'-(4-Methylumbelliferyl)- α -D-N-acetylneuraminic acid (4-MUNANA) was purchased from Sigma Aldrich (Catalog #M8639). MDCK-ULTRA culture media (Catalog #BW12749Q) and Cell Titer-Glo Luminescent Cell Viability Assay Kit (Catalog # PR-G7571) were purchased from Fisher Scientific.

Influenza Virus Infection

Influenza A (H1N1) stocks were grown from a single purified plaque and concentrated to 2×10^6 PFU/ml in 500 μ l aliquots and stored at -80°C. Individual aliquots were thawed as needed. All assays used an MOI of 0.05 to 0.08. Viral infection media was supplemented

with 1.0 ug/ml TPCK Trypsin prior to infection to aid in influenza cellular entry. Influenza viral growth assays were incubated at 37°C with 5% CO₂ for 72 hours. Determination of viral growth was based on the quantification of neuraminidase activity by measuring fluorescence of the cleaved substrate 4-MUNANA.

Primary High Throughput Screening

Ninety-six well plates were initially seeded with 5000 MDCK cells/well in 150 ul MDCK ULTRA media supplemented 1% antibiotic (100 U Penicillin/Streptomycin/ml).

After allowing 24 hours for cell adherence, each well was treated with 10 uM of a unique compound from SIGA's compound library. Plates were then infected with Influenza virus at 250 PFU/well for an MOI of 0.05. With the exception of the virus only (positive) and no virus (negative) control wells, 45 uM RBV (EC90) was also added to each well to inhibit viral growth. Virus was allowed to incubate for 72 hours post infection at 37°C with 5% CO₂.

Readout for this screen measures the neuraminidase activity (NA) in each well using 10 uM of the synthetic substrate 2'-(4-Methylumbelliferyl)- α -D-N-acetylneuraminic acid (4-MUNANA). Neuraminidase, a glycoside hydrolase, cleaves 4-MUNANA into 4-methylumbelliferone (4-MU) which can be measured fluorometrically. The amount of fluorescence per well is a direct representation of the NA activity, which is further correlated to the amount of virus present in the well. Comparison of this value to the virus only controls allows calculation of the percent viral growth per well.

After a one hour incubation at 37°C, NA hydrolase activity was quenched with the

addition of 150 ul stop solution (25% Ethanol and 75% 0.1M glycine pH 10.7). Fluorescence was excited at 350 nm and emission was measured at 465 nm using an Envision Plate Reader.

Secondary Screening

Hits from primaries were run in triplicate 7-point dilutions to measure the dose dependent response of the compound against an EC50 concentration of RBV and to measure cytotoxicity as a result of treatment (CC50). Cytotoxicity was measured in the absence of viral infection using Alamar Blue as an indicator of cellular metabolic health. These plates were read fluorometrically with an excitation of 570 nm and an emission of 600 nm and compared to cell only control wells to allow calculation of percent viability in each well. Viral growth in the EC plates was determined from NA activity on 4-MUNANA.

Tertiary Screen assay development

Cell density

Tertiary screening was moved into a 384 well format using MDCK cells in serum free MDCK-ULTRA media. The optimal seeding density was found using a 1:2 cell dilution series with 8 replicates per dilution. These were then incubated at 37°C for 120 hours. Determination of cell growth in the presence and absence of compound or virus was based on the amount of ATP/well measured with 25 uL/well Cell Titer Glo [13].

Influenza Virus Infection

A TCID₉₀ was conducted using a half-log 20 point dilution series beginning at a multiplicity of infection (MOI) of 2.4. Eight replicates were used at each MOI. The 4-MUNANA/NA readout was used as described previously in order to quantify viral growth.

Mutagen Antiviral Activity

Using the optimal cell density and viral concentration, multiple mutagens were tested in 20 point dilutions from 250 uM down to 1 uM with four replicates per concentration. Mutagens were dispensed using an HP D300 Digital Dispenser. Readouts used the 4-MUNANA/NA assay described above. Viral inhibition curves were then created using the relative neuraminidase activity per mutagen concentration compared to virus only controls. Cytotoxicity of each mutagen was quantified using Alamar Blue.

Antagonism Screening

The activity of compounds from secondaries was measured against multiple mutagens discovered from Tertiary screening in a 384-well plate format. Plates were seeded as previously described above with 5000 cells/well in 45 uL MDCK-ULTRA and after 24 hours were treated with a 7 point range of RBV dilution down columns 2-11 and 12-22 and then co-treated with a 10 point dilution of RIC compound across this dilution in rows B-H and I-O. This resulted in four 8x11 quadrants with each well representing a different combination of RBV and RIC-compound, and each row representing a dilution of RIC compound against a constant concentration of RBV. From this data an EC50

concentration of RIC-compound was found against seven different concentrations of RBV. The extra column (22) represented a RBV only control dilution in the absence of RIC and the extra rows (H and O) were a RIC compound control in the absence of RBV. “Virus only” and “no-virus” control wells were placed in columns 23 and 24.

EC plates were infected with influenza at an MOI of 0.05 and cytotoxicity plates were mock infected with 5 ul ULTRA supplemented with TPCK. Total assay volume was 50 uL/well.

Plates were incubated for 72 hours at 37°C. Viral growth in the EC plates was measured with 4-MUNANA and cell growth in the cytotoxicity plates was measured using Titer-GLO, 25 uL/well as specified by Promega.

Emergent Mutation Assay

Four white 384 well plates were initially seeded with MDCK cells at a density of 5000 cells/well in 45 ul of serum free MDCK-ULTRA media. After 24 hours each plate was treated with a different experimental condition. All wells of plate A were treated with 12 nM (EC50) Zanamivir (Zan); Plate B was treated with 1.92 uM RIC-2; Plate C was treated with both 12 nM Zanamivir and 1.92 uM RIC-2; and Plate D was treated with an equivalent concentration of DMSO to act as a virus only control. All plates were normalized to the same DMSO concentration of 1.12 uM. All wells were then infected with 150 PFU Influenza (MOI of 0.03). Virus was incubated for 72 hours at 37°C.

After 72 hours of viral growth samples from passage 1 wells were passed into fresh culture plates by diluting 2 ul from each well in the passage 1 plates into 198 ul MDCK

ULTRA. Two microliters of this dilution was then transferred to the corresponding well of the passage 2 plates. The passage 2 plates had been seeded 24 hours previous in a manner consistent with passage 1 plates and were treated as described above with the specified compound for each treatment group. In this way, virus from well A1 from passage 1 was diluted and transferred to well A1 of the passage 2 plate. The virus was thus serially passaged 4 times for a total viral growth period of 17 days in the presence of each treatment type. After each transfer of virus to the new passage plates, the viral growth in the preceding passage was fluorometrically measured using 4-Munana.

Pre-incubation for chemical interaction between RIC-1 series and Ribavirin

In order to rule out a direct chemical interaction between the RIC series and Ribavirin, the two compounds were added to “neat” media in a dilution plate and allowed to incubate for 6, 3 and 0 hours at 37°C. Each addition time point had 3 replicates of a 6 point range of RIC-1 concentrations (18.0 uM, 10.8 uM, 4.5 uM, 1.8 uM, 0.9 uM, and 0.18 uM) against 810 uM RBV. Additional treatment groups were, three replicates of 810 uM RBV incubated for six hours with 10.8 uM RIC-1 added at T=0, and three replicates of 10.8 uM RIC-1 incubated for 6 and 3 hours with 810 uM RBV added at T=0. In addition, there were three replicate wells of ribavirin only and RIC-1 only controls at each time point.

A 96 channel liquidator was used to transfer 10 ul from the 96 well dilution plate to two separate 96 well tissue culture plates which had been seeded with 5000 MDCK cells/well in 150 ul MDCK-ULTRA 24 hours prior. Plates were then infected at an MOI of 0.05 in a

final volume of 170 μ L. Since the dilution plate was concentrated the 1 to 17 dilution from the dilution plate to the 384 well assay plate resulted in the desired RIC concentrations of 1.0 μ M, 0.6 μ M, 0.25 μ M, 0.1 μ M, 0.05 μ M, and 0.01 μ M and a RBV concentration of 45 μ M RBV (EC90).

Infected cells were incubated as previously described for 72 hours and viral growth was measured using 4-MUNANA. All replicates were averaged and compared to virus only control wells for percent viral growth. Cell viability was measured using 100 μ L/well of Titer-Glo as specified by Promega.

Pre-incubation of RIC-1 and RIC-2 to measure rate of association

MDCK cells were seeded at 5000 cells/well in 150 μ L ULTRA media in 96 well plates. After 24 hours of incubation, cells were treated at different time intervals with three replicates of a 5 point dilution of RIC-1 ranging from 1.5 μ M to 0.05 μ M. A separate plate was treated in the same way with RIC-2 ranging from 3.0 μ M down to 0.1 μ M. Compounds were added at time points T = -4.5 hours, -60 minutes, -30, -15, -5, and -2.5 minutes. All plates were then rinsed thoroughly four times with 200 μ L cold DPBS to remove any trace of non-bound RIC. Individual washes consisted of multiple “pipetting up and down” steps in order to physically rinse the monolayer. Cells were again covered in 150 μ L MDCK-ULTRA.

The same 5 point dilutions of RIC-1 and RIC-2 were added in duplicate to the remaining untreated wells. To act as a control all wells were then treated with 45 μ M RBV, with the exception of virus only and cell only controls.

Plates were infected with influenza as specified in primaries and viral growth was measured after 72 hours using 4-MUNANA. Duplicate plates were carried without infection and cell viability was measured using Alamar Blue.

Ribavirin Uptake

Six well plates were seeded with 1.2×10^6 MDCK cells per well in 2 ml MDCK-ULTRA and incubated at 37°C for 24 hours. Using one plate per sample group, six treatments were used; 150 uM RBV, 750 uM RBV, 1500 uM RBV, 150 uM RBV with a long wash, 150 uM RBV + 5 uM RIC-1, and 150 uM RBV + 50 uM NBMPR. Plates were first incubated with RIC-1, NBMPR, or a media control for 1 hour to attain complete activity. Ribavirin was then added to all plates and incubated for 20 minutes to allow equilibration into the cell. The media from all wells was removed and the monolayers were washed with 1 ml 4°C DPBS for 4 seconds to remove extracellular RBV. The “long wash” samples received two separate 30 second washes with 4°C DPBS. Half the wells were then lysed with 600 uL acetonitrile for 2 minutes followed by disruption of the monolayer with a cell scraper. This volume was then aspirated from each well and transferred to a second well of the same treatment group in order to collect cells from two wells into the same 600 uL volume. Each six well plate therefore resulted in three unique replicates each consisting of cells collected from two wells. The RBV concentration in each sample was measured using mass spectroscopy against an internal standard.

Interaction of RIC series with the inhibition of the IMPDH pathway

Using the “four quadrant 384 well” format previously described in the “antagonism screening” a dilution of RIC-1 was tested against multiple concentrations of the IMPDH inhibitor Mycophenolic Acid (MPA). Influenza growth in each well was based on neuraminidase activity in comparison to the virus only controls. Duplicate uninfected plates were carried as a measure of cytotoxicity using Cell Titer Glo. Compounds were dispensed using an HP D300 Digital Dispense instrument.

Results

High-Throughput Screening

Primary screening of SIGA's compound library against a viral infection artificially inhibited by the addition of 45 uM Ribavirin revealed a compound series that reversed the antiviral effect of RBV resulting in the return of viral growth to control levels. This series consisted of hundreds of individual compounds each composed of a conserved core structure consisting of “purine nucleoside-like” fused ring structure. Differences between each compound within the series were limited to substitutions, additions, or subtractions of side groups attached to the central structure. These modifications resulted in an altered degree of activity against RBV. Further testing in secondary screening verified the initial hits with an eight point dilution, providing an approximate EC₅₀ value for each compound (data not shown). The lead compounds from this series were then tested in a 20 point dilution against variable levels of RBV for an established EC₅₀ value at each RBV concentration. Figure 1 shows inhibition values of RIC against an EC₉₀ concentration of RBV. The two lead compounds, RIC-2 (EC₅₀=0.3 uM) and RIC-1 (EC₅₀=0.11 uM), were further used as representative compounds for the series in order to better understand their mechanism of action. Both compounds had the conserved central ring structure seen throughout the RIC series with structural alterations made only to side compounds. Due to the conserved structure and their high activity these compounds were decided to be representative of the series in future testing.

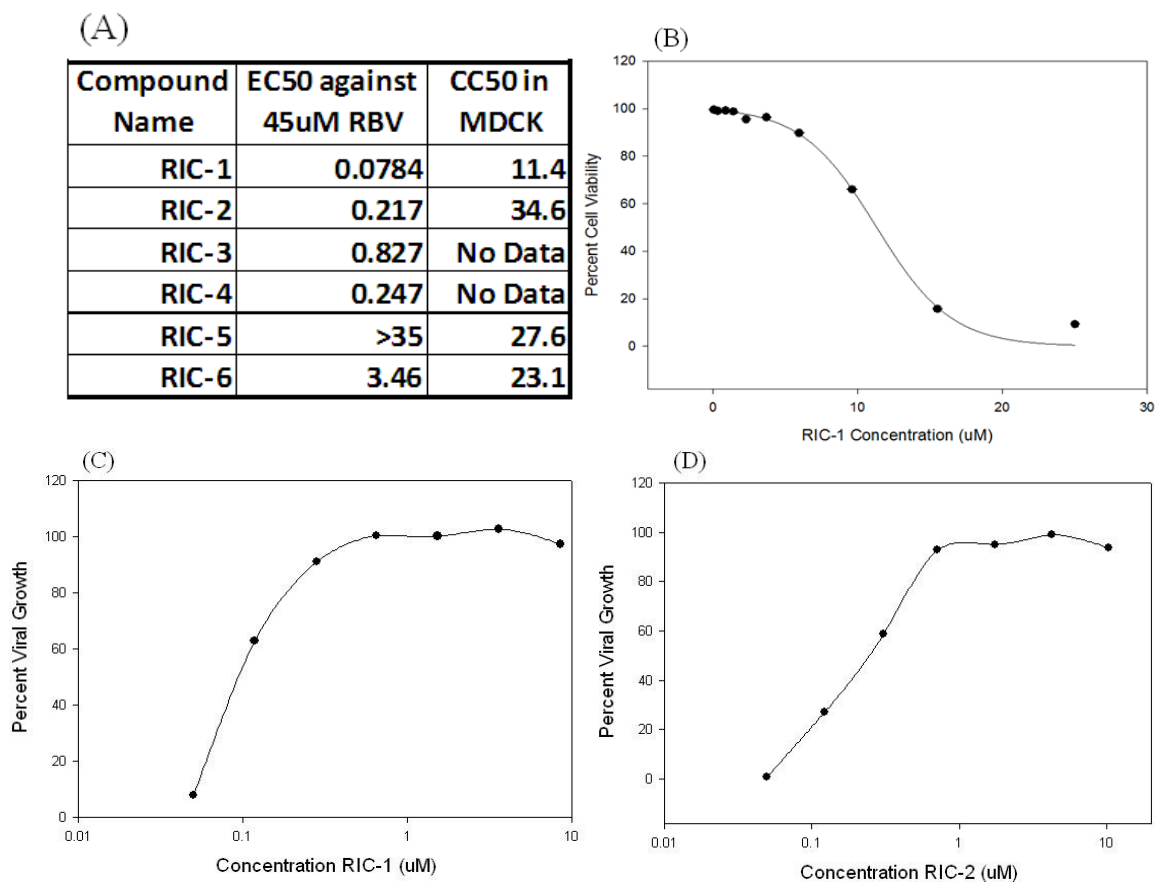


Figure 1: Ability of Lead compounds to return Influenza growth after treatment with 45 uM RBV. Panel A Six of the top compounds identified from primary HTS screening (uM) were diluted against 45 uM (EC90) RBV to quantify their reversal of RBV's antiviral activity in H1N1. Viral growth was determined based on the degree of neuraminidase activity after a 72 hr incubation. **B:** Cytotoxicity of RIC-1 on MDCK cells was determined in the absence of viral infection and used cellular ATP levels measured with Cell Titer-Glo as a determination of cell viability. **C.** Inhibition of RBV's antiviral activity by RIC-1. **D.** Inhibition of RBV by RIC-2. All data points represent the average of 4 replicates each compared to the cell only controls (0 uM RIC-1).

The intent of the high throughput screen was to use RBV as a viral mutagen thereby artificially pushing the RDRP past the error threshold with the intent of identifying compounds that could return viral growth via an increase in RDRP fidelity. However, due to the uncertainty concerning the antiviral mechanism of RBV in influenza, four main possibilities were subsequently tested to better understand the mechanism by which the RIC series inhibits RBV (Figure 2).

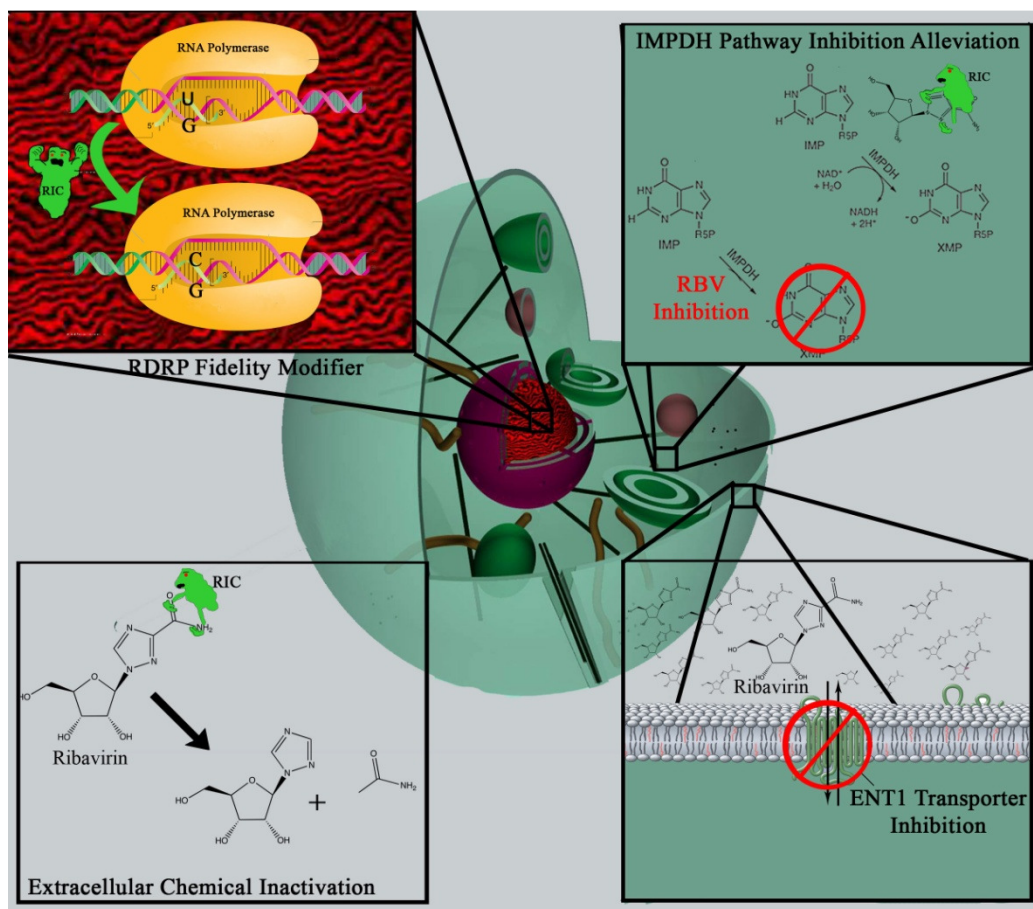


Figure 2 Possible sites of interaction between the RIC compound series and RBV. Four possible sites of interaction were investigated for possible involvement in the anti-Ribavirin activity demonstrated by the RIC series. The intended function of RDRP fidelity (upper left), alleviation of IMPDH inhibition by RBV thereby returning a normal distribution of nucleotide pools (upper right), inhibition of ENT-1 preventing cellular uptake of RBV (lower right), or by a direct chemical inactivation of RBV by the RIC series (lower left).

RBV specificity testing using multiple nucleoside analogs

To assess whether the alleviation of viral inhibition was caused through an increase in the fidelity of the viral RDRP or if the compound series was acting in a RBV specific manner, independent of any polymerase involvement, RIC-2 was tested against various other nucleoside analogs. Nucleoside analogs have shown the most promise in decreasing the RDRP fidelity and pushing viral populations past the error threshold [21].

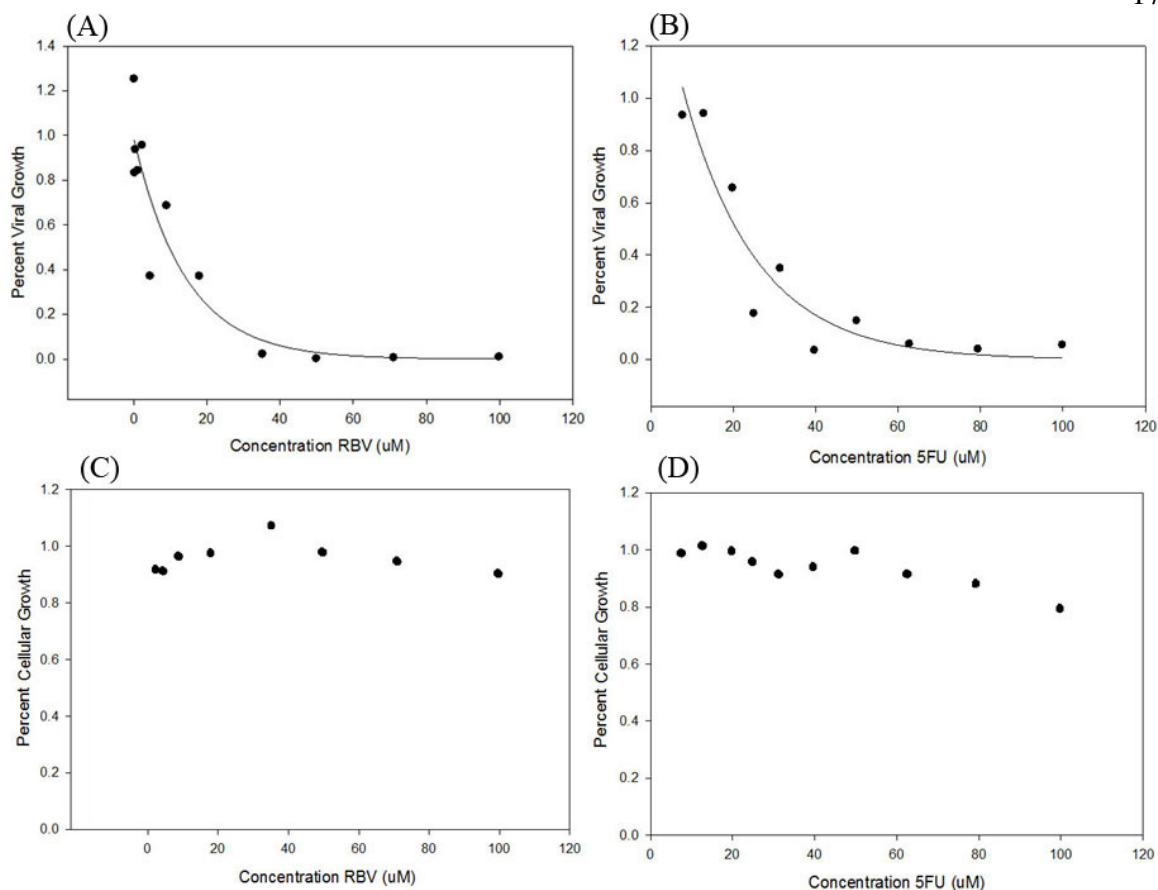


Figure 3. Inhibitory effect of Ribavirin and 5-Fluorouracil on Influenza. Of the six tested, two nucleotide analogs, RBV and 5FU, demonstrated an ability to inhibit viral growth (A and B). Ribavirin showed greater efficacy with an EC50 around 10 uM compared to an EC50 of 20 uM for 5FU. No cytotoxicity was seen for RBV at the concentrations tested (C) while 5FU showed minor cytotoxicity associated with a 20% drop in cellular ATP levels at 100uM (D). Cell viability was determined using Cell-Titer Glo to measure the amount of ATP/well which was then compared to the average ATP/well from the cell only controls. Values for EC's and CC's represent the average of four replicates

The efficacy of RIC-2 against multiple analogs would suggest a mechanism of action that was not specific to RBV. Excluding a RBV specific mechanism of viral population rescue would support the RIC series acting to increase RDRP fidelity thereby saving the virus from an error catastrophe.

Multiple nucleoside analogs were tested including Azacytidine (AZT), 6-Mercaptopurine (6MP), Fludarabine phosphate (FAF) and Thioguanine (TG); only the analog 5-

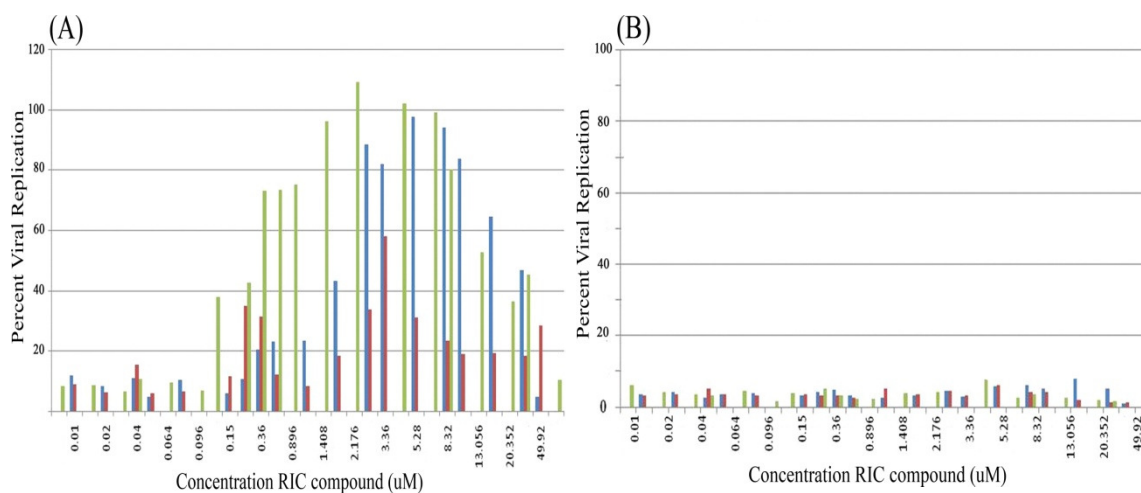


Figure 4. Comparison of RIC-2's ability to relieve viral inhibition resulting from treatment with either RBV (A) or 5FU (B). Three RIC-compounds, RIC-2 (Green), RIC-6 (Blue) and RIC-5 (Red) were tested for their ability to reverse the effect of multiple nucleoside analogs in a concentration dependent manner. Values represent the average from 4 replicates at each concentration. Percent viral growth is calculated as relative neuraminidase activity in comparison to the average of 10 virus only control wells.

Fluoruracil (5FU) successfully inhibited influenza growth with an EC50 value of 20 uM (Figure 3B). No cytotoxicity was seen at this concentration but testing up to 100 uM 5FU resulted in a moderate 18% decline in cellular viability (Figure 3D). Azacitidine showed complete cytotoxicity at 6 uM, while concentrations up to 250 uM of 6MP, FAF and TG demonstrated no effect on influenza growth after 72 hours.

Three of the first compounds identified in the RIC series, RIC-2, RIC-5, and RIC-6, were tested against an EC90 concentration of RBV and then an EC90 concentration of 5FU to measure their ability to relieve viral inhibition by both mutagens. All three compounds demonstrated a dose dependent increase in viral growth against RBV treated cells with compounds RIC-2 and RIC-6 able to completely rescue viral growth (Figure 4A). In contrast, this result was not seen when the three RIC compounds were diluted against 5FU (Figure 4B). The viral growth remained constant at 5-15% and did not demonstrate a

dose dependent response at any concentration of RIC compound. Viral growth inhibited by 5FU was not influenced by any of these three compounds. These data suggest the compound series alleviates RBV viral inhibition in a manner separate from viral inhibition caused by 5FU.

Emergent Mutation Assay

In an environment without a selecting pressure, mutations occur randomly at a constant rate. The large population size of diverse variants all randomly mutating would result in little phenotypic alteration in the viral population [7]. The addition of Zanamivir acts as a selective pressure to preserve variants with acquired resistance to Zanamivir. Since the virus's ability to gain resistance is dependent on the low fidelity of its RDRP, compounds that increase the fidelity will slow or prevent the development and enrichment of emergent variants that are resistant to Zanamivir. The rate at which a viral population of influenza acquired resistance to the antiviral Zanamivir was measured in the presence and absence of RIC-2.

If RIC-2 increased polymerase fidelity we would expect to see a decrease in the rate of acquired resistance, resulting in continued growth inhibition throughout all passages.

Since each well was passaged separate from the others each passage had 384 unique viral populations. The amount of viral growth in each well was measured for all 4 passages and compared to the virus only control DMSO plate. In this way the variation in the viral growth in each well was measured over four passages. Viral growth per well was sorted into 20% ranges of growth and separated based on passage number. The distribution of viral growth based on treatment type is shown as a histogram in Figure 6.

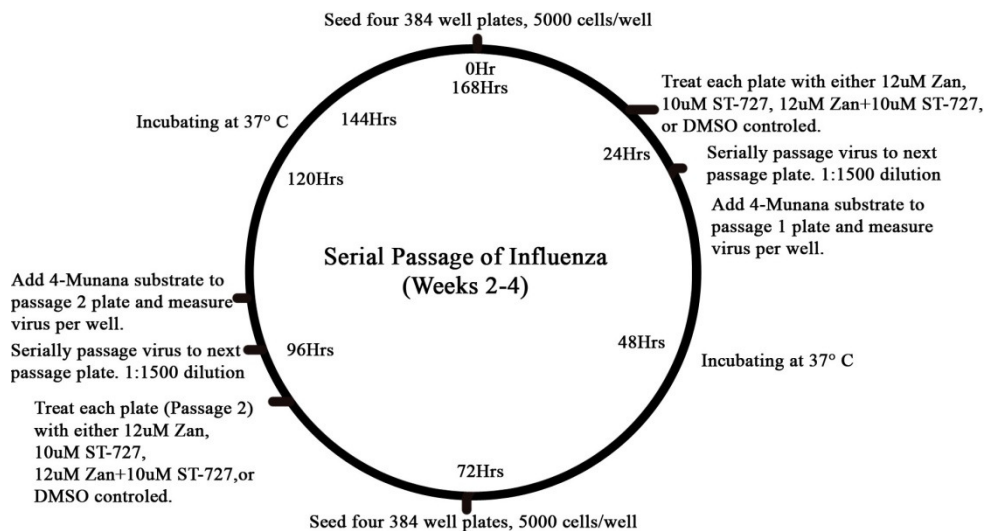


Figure 5. Cyclic serial passage treatment plan for selection of Zanamivir resistance in Influenza. Using a uniformly treated 384 well culture plate for each group (MDCK cells), four treatment groups consisting of a DMSO control, Zanamivir only (EC50), RIC-2 only (1.92 uM), and RIC-2+Zanamivir were serially passaged twice a week. Passage 1 plates were directly infected with stock Influenza at an MOI of 0.05. Each consecutive passage was infected with a dilution of the supernatant from the preceding passage. Neuraminidase activity per well was measured in the preceding plate, after viral transfer, as a measure of viral growth. In this way, 384 viral populations/treatment were grown for 17 days.

The neuraminidase activity per well is compared to the average amount of neuraminidase activity per well from the DMSO passage plates which were set as “100% viral growth” for all plates in that particular passage.

The DMSO only control plate showed a consistent Gaussian distribution over all four passages centered around 100% viral growth. Treatment with “RIC-2 only” demonstrated a similar distribution as the DMSO control group for all passages (data not shown). Since RIC-2 does not act on viral growth alone but rather prevents an inhibition of growth due to treatment with RBV, treating virus with RIC-2 alone was not expected to affect viral growth rates. A small portion of the DMSO only group (14 wells) ended with less than 20% growth in passage four. These wells were randomly distributed throughout the plate

and are interpreted to be lost due to procedural techniques. Transfer of virus from plate to plate using a small sample of the supernatant induces some inconsistency in the exact number of PFU's transferred. Fourteen wells after 4 passages are therefore considered the likeliness that any well might be lost due to the experimental design rather than by treatment with Zanamivir in the other two plates.

Passages 1 and 2 of the "Zan-only" treated plate showed slightly rightward weighted Gaussian distributions (Figure 6). Passage 1 had a mean value of 51.4 percent while passage two had a mean of 55.1 percent viral growth. Passage 1 of the cotreated plate showed a leftward weighted Gaussian with a mean value of 55.5 percent. Passage 2 showed a more standard Gaussian distribution with a mean of 41.1 percent viral growth. The Gaussian distributions of viral growth are indicative of populations that exist with naturally occurring genomic heterogeneity. Due to its large size, the initial stock viral population will inherently consist of some variants with a modified sensitivity to Zanamivir. An EC50 value of Zanamivir therefore represents the concentration at which the population as a whole resulted in 50 percent viral growth. The distribution around the 50 percent value initially depends on the range of Zanamivir susceptibility of each variant present. As seen in the first passage of Figure 6 a very small percent of the wells demonstrated 100% viral growth indicating a number of variants in the original population conveyed a complete resistance to the EC50 concentration of Zanamivir. These variants were immediately able to replicate at a normal rate. A redistribution of growth is seen in passages 3 and 4 with Zan-only and the cotreated viral populations moving to broadly occupying all

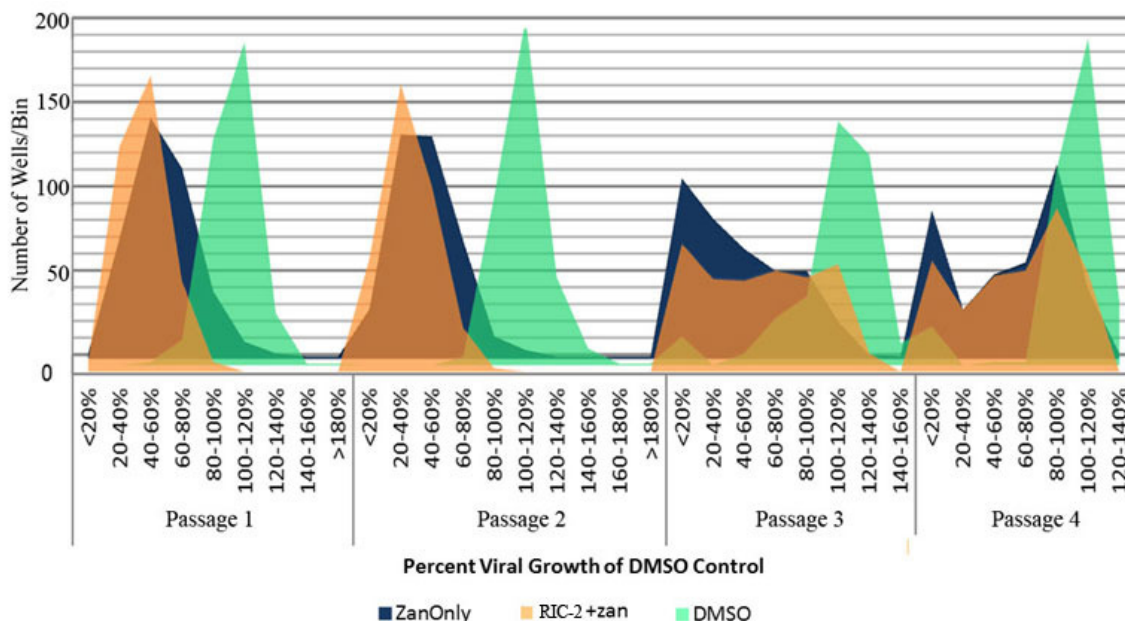


Figure 6. Histogram showing effect of RIC-2 on the distribution of viral growth after serial passage in the presence of Zanamivir. The neuraminidase activity in each well was compared to the average value of the DMSO only plate resulting in the percent viral growth for that well. Using the calculated viral growth per well, 384 populations per treatment were separated into bins representing a 20% range in viral growth. The total number of wells in each 20% interval is shown.

percentiles in a bimodal distribution by passage 4.

Passage 3 of the cotreated plate had substantial representation across all percentiles (<20% to 100-120%) with a 22 well range between the most and least populated states. A single peak of 104 wells at <20% viral growth was present with a gradual rightward decline into the higher growth range. The overall trend seen in the transition from plate 2 to 3 is a shift of viral populations into areas of increased viral growth seen by the redistribution into more heavily populated percentages. This redistribution of viral populations into the bins of higher growth is seen to continue into passage 4 resulting in a bimodal distribution. Both the “zan-only” and the cotreated plate demonstrate an increase in the number of populations over 80% viral growth. A major viral growth peak at is seen

in both treatment groups centered around 80%-100% with over two-thirds of each population over 50% viral growth. A small subset of each population demonstrated significant inhibition of viral growth resulting in a minor peak seen <20% growth. Viral populations from both zan treated samples demonstrated a highly similar distribution despite treatment with RIC-2 suggesting RIC-2 does not influence viral growth in the presence of Zanamivir.

After four passages no variation was seen in the distribution of viral populations between the Zanamivir only and the group treated additionally with RIC-2. Both groups rapidly and equally experienced a shift in the viral population from a single normal distribution centered around 50% growth to a bimodal distribution with peaks centered around 20% and 80%. Passage 4 of the Zan-only group had 84 wells under 20% viral growth and 166 wells over 80-100% viral growth. Similarly the co-treated plate finished with 53 wells under 20% and 156 wells over 80% growth.

As expected, treatment with the antiviral Zanamivir initially resulted in an inhibition of viral growth which was eventually overcome after 17 days of viral growth. Treatment with RIC-2 did not appear to alter the rate of acquired resistance as both the zan only and cotreated plate demonstrate identical shifts. Furthermore, the number of populations demonstrating an increase in viral growth is also identical despite treatment with RIC-2. Both plates treated with Zan ended with equal portions of the total population growing to over 80% viral growth

Preincubation of RBV with RIC-1 to measure for a direct chemical inactivation of RBV

A chemical interaction, occurring independent of cellular activity, between RBV and

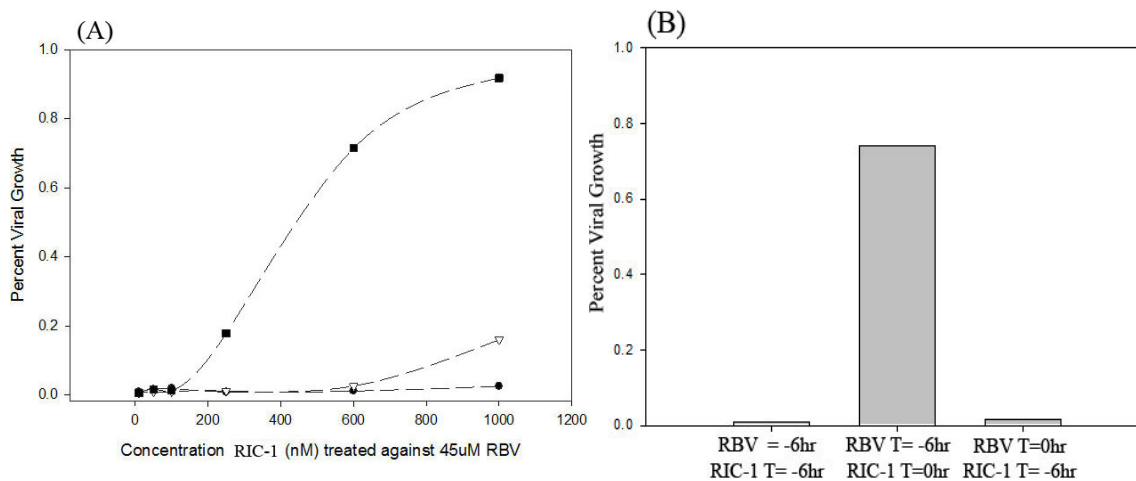


Figure 7: Effect of Preincubation on the RIC-1/RBV interaction. A dilution of RIC-1 was preincubated in MDCK-ULTRA media at 37°C for either 6 hours (circles), 3 hours (triangles) or 0 hours (squares) before being added to MDCK cells infected with Influenza (A). Neuraminidase activity was measured after a 72 hour incubation and compared to virus only control providing a percent viral growth in each well. Furthermore, both compounds were preincubated separately for 6 hours and then tested against each other and against the opposite compound that had not been preincubated (B). Points are an average of 3 replicates.

RIC-2 could result in an alteration of the chemical structure of RBV, causing an inhibition of RBV's mechanism of action either by preventing cellular uptake, altering binding to its target site, an increased instability, or by decreasing solubility leading to precipitation.

A concentrated range of RIC-1 concentrations were incubated with 17x RBV in "neat" serum free MDCK-ULTRA media for 6 hours and 3 hours. At t=0 aliquots of the media containing the preincubated compound combinations were transferred to a tissue culture plate in order to treat them with the correct concentration of preincubated RBV and RIC-1. This tissue culture plate was then infected with influenza. Viral growth in these samples was compared to viral growth in cells treated with RIC-1 and RBV that had not been preincubated. If RIC-1 were directly chemically interacting with RBV prior to cellular entry it could render RBV inactive and explain the reversal in antiviral activity. If

this were true, then preincubation of the two compounds should result in a decrease in the effectiveness of RBV, with longer preincubation times resulting in greater viral growth. A six hour preincubation did not result in greater viral growth and in fact maintained a complete inhibition of virus (Figure 7a). Three hours of incubation resulted in only the highest RIC-1 concentration showing a modest 18% reversal of RBV activity, compared to the 92% reversal of RIC-1 added at T=0. The complete inhibition of viral growth at six and three hours indicates full functionality of RBV when incubated with RIC-1 for these durations.

When the two compounds were immediately added to cell culture without preincubation, RIC-1 demonstrated a typical dose dependent reversal of RBV. In comparison, the six hour preincubation showed complete viral inhibition by RBV suggesting a loss of functionality of RIC-1.

Furthermore, RIC-1 incubated alone in neat media for 6 hours and then tested against RBV, which had not been preincubated, again showed inhibition of viral growth (Figure 7b). The antiviral effect of Ribavirin, preincubated alone for six hours in media, was reversed with the addition of RIC-1, which had not been preincubated; indicating fresh RIC-1 was capable of interacting with preincubated RBV, while preincubated RIC-1 is not (Figure 7b). Taken together, these data indicate a decrease in the activity of RIC-1 with increasing preincubation times, possibly resulting from instability of RIC-1 at 37°C. No loss of function in RBV was seen due to preincubation with RIC-1 indicating the interaction between RIC-1 and RBV does not occur through an extracellular chemical inactivation of Ribavirin.

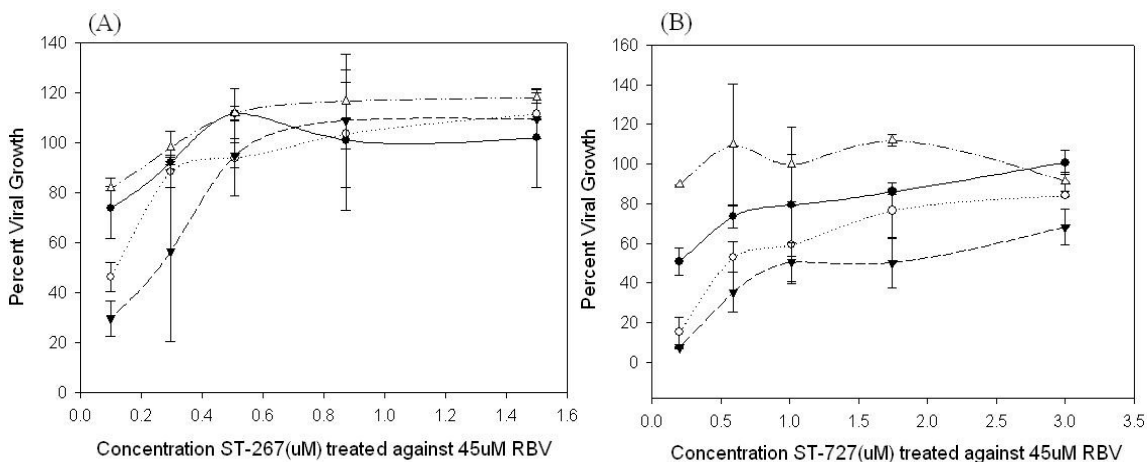


Figure 8. Effect of short incubation times on efficacy of RIC-1 and RIC-2 in inhibiting 45 uM RBV: Triplicate five point dilutions of either RIC-1 (A) or RIC-2 (B) were incubated with cells for decreasing amounts of time (60 minutes=solid line w/ closed circles, 15 minutes=dotted line w/open circles, 2.5 minutes=dashed line w/ closed triangles, and Control added after wash=dashed/dotted line w/open triangles). Cells were then rinsed thoroughly with cold DPBS to remove any unreacted compound and new growth media was added. Activity against 45 uM RBV was measured based on the ability to return viral growth to control values after 72hr incubation. Viral growth was based on measured neuraminidase activity.

Rate of Association between RIC-1 and its Target Site

The antiviral nature of RBV is dependent on multiple generations of virus. As a result, all screening measured viral growth 96 hours after the addition of RBV and RIC-1 treatment. Paradoxically, RIC-1 showed an apparent instability at 37° C with an almost complete loss of function in 3 hours. Somehow RIC-1 was able to inhibit RBV for the entire assay long after it should have degraded due to instability.

To understand the kinetics of RIC-1 activity, the rate of association between RIC-1 and its target were measured by decreasing the duration of treatment with RIC-1. Rather than leaving the RIC compound in the well for the entire assay, as we had previously done, after the desired incubation time, the cell monolayer was rinsed to remove all unreacted RIC-1. Cells were then treated with 45 uM RBV and infected in new growth media lacking any additional RIC-1, insuring only RIC-1 utilized during the initial incubation

was available to act antagonistically to the continuously present RBV. In order to establish a positive control for RBV inhibition a portion of the plate was treated with a dilution of RIC-1 without washing. RIC-1 at 0.5 μM or higher demonstrated the ability to completely inhibit RBV at all incubation time points down to 2.5 minutes (Figure 8a). A time dependent loss of functionality was seen at decreased concentrations. This loss was seen with decreasing incubation times experiencing a larger decline in RIC function at concentrations below 0.5 μM RIC-1 (Figure 8a). Treatment with RIC-2 showed a partial loss of functionality even at the highest concentration tested, with only 3.0 μM for a 60 minutes incubation resulting in complete RBV inhibition. Decreasing the duration of incubation resulted in linear loss in activity at the higher concentrations but an increasing decline in function at the lowest concentrations of RIC-2.

These data suggest that the loss of function of the RIC series when incubated in media at 37°C is avoided due to a rapid interaction with the cell. Incubating the cells with 1 μM RIC-1 for 2.5 minutes resulted in a complete inhibition of RBV for the full 72 hour assay indicating a rapid utilization of the compound and resulting in a prolonged anti-ribavirin effect. These results may be explained by either a quick association with the target of action resulting in a long lasting alteration of function or through a rapid uptake and a prolonged intracellular stability. RIC-2 demonstrated a less efficient utilization by the cell. Due to the structural similarity and approximate size between RIC-1 and RIC-2 these data suggest a dramatic alteration in the rate of interaction due to small chemical modifications.

Cellular Uptake of RBV

While Ribavirin's MOA is unclear, inhibition of RBV uptake by the cellular Equilibrative Nucleoside Transporter 1 (ENT-1) results in a form of resistance to the antiviral effects of RBV [41,42]. Cellular uptake of RBV is mediated solely by ENT-1 and ENT-2 with transport via ENT-1 accounting for the majority of the uptake [41]. Inhibition of ENT-1 by the RIC series would block the cellular uptake of RBV and subsequently prevent the viral growth inhibition caused by RBV.

To assess whether treatment with RIC-1 could alter cellular uptake of RBV we measured the amount of RBV in cell samples pretreated with RIC-1, the ENT-1 inhibitor NBMPR, or with neat media (control) prior to a 20 minute incubation with RBV. The cell monolayer was then collected in acetonitrile and the concentration of RBV in the cell suspension was determined using Mass Spectroscopy to quantitatively measure the amount of internalized RBV.

Multiple concentrations of RBV were used in order to establish a correlation between the measured RBV levels and the concentration used in treatment. The measured RBV concentration in the 1x, 5x and 10x "RBV only" samples returned values of 1774 ng/ml, 6765 ng/ml and 10,770 ng/ml respectively (Figure 9), verifying that measured RBV concentration varies with the treatment concentration.

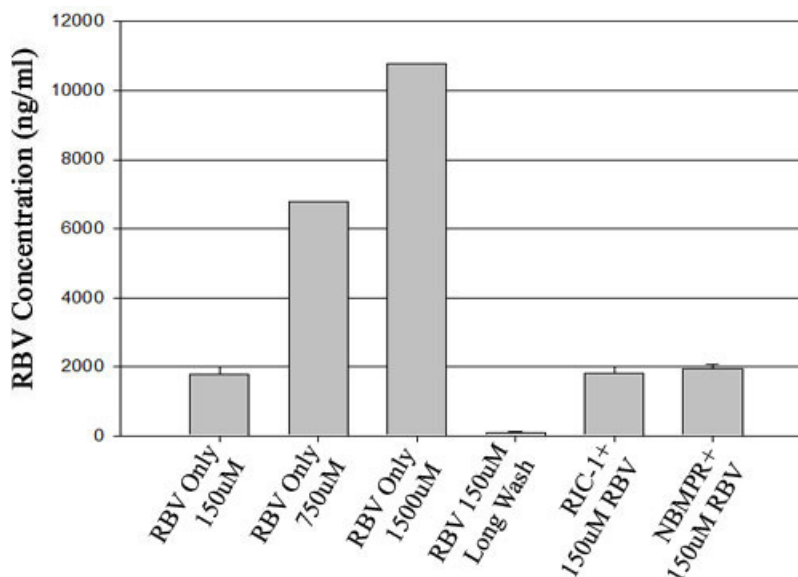


Figure 9. Cellular uptake of RBV (inferred to be mainly by ENT-1) in the presence of RIC-1. MDCK cells were incubated with RIC-1, NBMPP, or a media control for 1 hour before a 20 minute incubation with 150 uM RBV. After a 4 second rinse with ice cold DPBS the cell pellet was collected in acetonitrile and the RBV concentration was measured using mass spectrometry. Data points represent the average value of 3 replicates with two wells from a homogenously treated 6 well plate combined for each replicate. The 750 uM and 1500 uM RBV samples represent one replicate consisting of two combined wells. The long wash consisted of two separate 30 second rinses with cold DPBS.

One of the samples treated with 150 uM RBV received a long wash in cold DPBS with the intent of allowing time for the equilibration of RBV out of the cell to demonstrate free movement both in and out of the cell. This sample resulted in 83.4 ng/ml approximately one and a third logs below the short wash samples.

Contrary to expectations, the sample treated with the ENT-1 and ENT-2 inhibitor, NBMPP, resulted in 1955 ng/ml representing a slight increase compared to the RBV only sample. Treatment with 50 uM NBMPP is shown to completely inhibit RBV uptake by ENT-1 and ENT-2 resulting in no intracellular uptake of RBV and therefore should act as positive control for the experiment. An equal concentration of RBV in both the positive and negative controls seriously calls into question the validity of the data. For this reason

it cannot be conclusively stated whether the measured RBV was intracellular, extracellular or membrane bound. However, a second experiment using a viral growth readout (data not shown) to measure NBMPR's effect on RBV also showed the NBMPR stock has a complete lack of activity against RBV. Despite treatment with NBMPR there was a continued complete depression of viral growth due to the RBV activity. These results combined could suggest an inactivity of the NBMPR stock rather than necessitating an invalidation of the results obtained from the uptake experiment.

The sample pretreated with RIC-1 had a RBV concentration of 1826 ng/ml in the cell pellet representing a 52 ng/ml increase compared to the RBV only sample. While the failure of the positive control makes a conclusion from this data difficult, an approximately equal amount of RBV was measured despite treatment with RIC-1. Since RIC-1 actively inhibits RBV in a viral readout it can safely be concluded that RIC-1 was active in the uptake assay as well. If the mechanism of action were through inhibition of the ENT-1 transporter we would expect to see a dramatic decrease in the measured amount of RBV.

RIC involvement with the IMPDH Pathway

One possible mechanism of action attributed to RBV is through inhibition of the IMPDH enzymatic pathway preventing de novo synthesis of guanine nucleosides. The resulting imbalance of nucleotide pools in the cell would lead to an increase in the number of incorrectly incorporated bases and an eventual error catastrophe. In order to determine a possible interaction between RIC and IMP

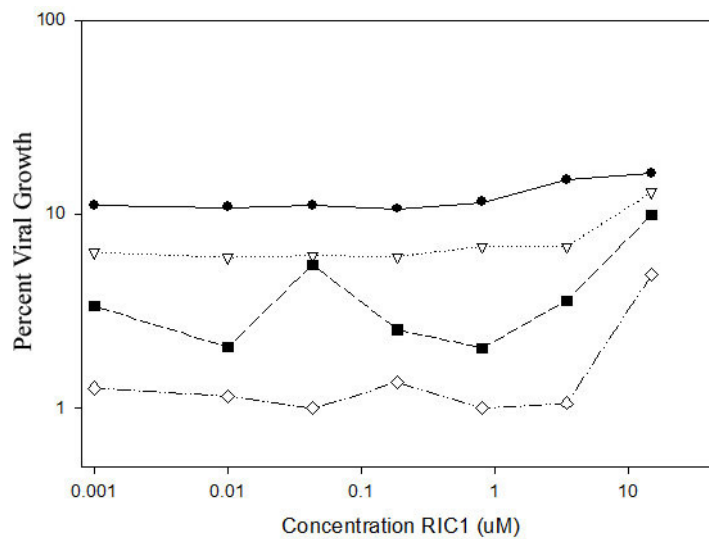


Figure 10. Effect of RIC on IMPDH inhibition by Mycophenolic Acid (MPA). Viral growth was inhibited by treatment with multiple concentrations of MPA and then treated with a 7 point dilution of RIC-1 (0.0 uM to 15 uM). Data points represent an average of 4 replicates. Neuraminidase activity per well was compared to average activity from 8 virus-only control wells to establish the percent viral growth. The MPA concentrations used were; 102 uM (diamond w/dashed-dotted line), 52 uM (squares w/dashed line), 13 uM (triangles w/dotted line), 1.8 uM (Circles w/solid line).

dehydrogenase we tested the ability of RIC-1 to alleviate inhibition of the IMPDH enzyme due to treatment with the IMPDH inhibitor mycophenolic acid (MPA).

As expected, treatment with higher levels of MPA resulted in a greater depression of viral replication with 102 uM MPA resulting in almost complete inhibition. Increasing amounts of RIC-1 did not produce a dose dependent increase in neuraminidase activity. Viral growth remained uniformly inhibited by MPA at all concentrations of RIC-1 used with a similar increase in growth of approximately 4% seen at 15 uM across all dilutions of MPA. Since the viral growth increase occurred equally across all MPA concentrations it is concluded to be a result of cytotoxicity of the 15 uM RIC-1. As seen in Figure 1b, 15 uM RIC-1 results in an 80% loss in cell viability. This increased cellular stress likely resulted in the surviving cells becoming more vulnerable to viral infection.

Discussion

While many compounds are available for the treatment of bacterial infections and pathogenesis, few exist that are capable of long term management of riboviruses. The characteristically low fidelity of the RDRP used by riboviruses coupled with their large population size creates a swarm of genotypically unique variants requiring an antiviral compound to be effective not only against all present variants but also against any future mutations [43,44]. The overall fitness of a riboviral population is therefore closely tied to the fidelity of its RDRP. Limiting the mutation rate of the RDRP is highly detrimental to the virus's overall replicative fitness and results in a genotypically homogenous population. Compounds which increase the polymerase fidelity therefore may represent a viable therapeutic option for the treatment of RNA viruses when used concurrently with current antivirals. By limiting the rate of mutation, viral species would be unable to mutate in response to both medically prescribed compounds and the immune response making them more susceptible to treatment.

Our goal was to identify compounds capable of increasing the fidelity of the Influenza A H1N1 RDRP using high throughput screening against a viral infection artificially depressed by the mutagen Ribavirin. High throughput screening revealed a compound series capable of reversing the antiviral effects of RBV at sub micro-molar concentrations. The intent of this screen was to identify compounds that increased the fidelity of the RDRP thereby limiting the mutation and adaptation rate of RNA viruses which would have the end result of creating a genetically homogenous and stable population with lowered fitness and a greater susceptibility to antiviral treatment. The

nucleoside analog RBV is shown to act antagonistically to viral growth and has been suggested to do so through an increased mutation rate causing an error catastrophe in the replication of the viral genome. A compound which increased the fidelity of the RDRP would be more resistant to the mutagenic effects of RBV by decreasing the chance of incorporating an incorrect nucleotide or nucleotide analog.

The HTS screen identified the RIC compound series as being capable of inhibiting the antiviral effects of RBV in cell culture. In order to screen out hits with RBV specificity, initial follow-up screening focused on using other mutagenic nucleoside analogs in order to establish efficacy of the RIC series against multiple analogs. Activity of the series against multiple analogs would suggest a broad spectrum MOA, while inactivity against all but RBV would strongly suggest a RBV specific activity. Further testing indicated the RIC-series was not effective against a second nucleoside analog 5-Fluorouracil. The identification of only one other analog inhibitory to viral growth drastically decreased the conclusiveness of this test. While inactivity of the RIC-2 series against 5FU may support a possible RBV specific MOA, an equally valid explanation is a selective increase in fidelity. That is, the series does function as a fidelity modifier but is not effective against 5FU. Ribavirin's structure is analogous to a purine while 5FU is similar to pyrimidines. The RIC-2 series may only functionally enhance RDRP fidelity in regards to the insertion of purines into the elongating chain while not affecting the selectivity for pyrimidines. Without testing against other “purine-like” mutagens or even a greater number of analogs, the series’ inability to inhibit 5FU is inconclusive.

In order to move toward a more natural setting for which the drug was intended, the rate

of developed resistance to the antiviral Zanamivir was measured in viral populations treated with RIC-2. The initial Gaussian distributions centered on 50% viral growth are a testament to the heterogeneity of the original viral stock (Figure 6). Each randomly created variant carries with it a unique sensitivity to the Zanamivir treatment resulting in a normal distribution in growth. The bimodal distribution after 17 days indicates approximately a quarter of the wells in both “zan-only” and “zan+RIC-2” were incapable of viral growth. In these wells none of the variants initially present and none of the subsequent mutations were able to survive in the presence of Zanamivir. A small portion of the DMSO control also demonstrated less than 20 percent viral growth. The majority of these wells showed a complete lack of neuraminidase activity and are assumed to be “lost” wells due to procedural techniques used in the serial infection.

A dramatic increase in the number of wells with over 80% viral growth is seen after only 17 days of growth. Due to the large number of wells it is concluded that the demonstrated resistance derives from emergent mutations in newly formed variants over the course of the experiment rather than by enrichment of preexisting resistant variants. The H1N1 genome is approximately 13,820 nucleotides long [51]. As there are 3 possible mutations at each site expression of every point mutation would take 41,000 different variants and expression of all mutants with unique sets of 2 mutations would take hundreds of thousands of unique variants. Realistically there could exist millions of unique clones in a given viral population, only some of which offering Zanamivir resistance. The low frequency of functional mutants with increased Zanamivir resistance makes it unlikely that 50 wells each initially received at least one resistant variant. As seen in the original

passage some wells initially showed 100% viral growth indicating they did in fact receive variants conferring complete resistance. However, the 1-2 wells per plate are within the expected frequency. Furthermore these wells show that if a resistant variant were initially present in each of these 100+ wells we should have seen complete viral growth in the first passage in each well. Instead, a gradual shift in the distribution of populations is seen moving from passage 2 to passage 4. Even after 7 days of growth very few wells in both the treatment groups have complete viral growth suggesting there are a limited number of wells containing variants capable of complete resistance.

The rate of acquired resistance was quicker than expected, however, and may indicate this experiment simply gave these variants a competitive advantage by inhibiting non resistant mutants. Assuming resistance virions were present in all wells initially, treatment with Zanamivir would hinder the growth of other variants allowing rapid growth of resistant genomes. However, in order to accept this explanation there would have had to be a prevalence of at least 1 variant demonstrating complete resistance in every 250 plated virions. Due to the genetic diversity demonstrated by RNA viruses we find this frequency to be a much more improbable explanation. For this reason the increase in wells over 80% growth is concluded to represent the development of emergent mutant variants not originally present in the initial viral stock. Deep sequencing approaches could be used in the future to verify this conclusion by comparing the genotypes from passage 1 and passage 4 and looking for any similarities or conserved sequences.

Throughout the experiment both “zan-only” and “zan+RIC-2” had nearly identical

population distributions. By passage 4 both treatments demonstrated significant resistance to Zanamivir in over half the populations. As it is concluded that the resistance demonstrated in passage 4 represents the emergence of new variants then these data suggest RIC-2 had no effect on the rate of acquired resistance. Since mutation rate is dependent on the fidelity of the viral RDRP, the equal rate of resistance suggests both treatment groups operated at equal fidelities. Coupled with the inability of RIC-2 to alleviate inhibition of 5FU these data strongly suggest a mechanism of action independent of RDRP fidelity modification.

The compounds, RIC-1 and RIC-2, were initially selected to be representative of the entire RIC series. This series is defined by a conserved core structure partially appearing similar to a purine-like fused ring. All compounds in the series demonstrating some degree of efficacy against RBV contain this conserved structure causing us to conclude it is necessary for the anti-RBV effect. RIC-1 and RIC-2 showed the most pronounced efficacy against RBV making them ideal for MOA studies. Due to their conserved structure with the RIC series we feel justified in generalizing conclusions determined using these two compounds to the entire RIC-series. Therefore, based on the results obtained we conclude the entire RIC series likely does not function via modification of polymerase fidelity.

While the RIC series does not appear to modify polymerase fidelity it still offered both a unique opportunity to study the effect of RBV on viral growth and also a possible insight into RBV's inhibition of viral replication. For this reason, the mechanism of action of the RIC series was further pursued. First, however, we wished to rule out a direct

extracellular chemical interaction between RIC and RBV resulting in a modification of RBV. Preincubation of RBV with RIC-1 in neat media for 6 hours prior to their addition to cell culture did not affect RBV's antiviral activity (Figure 7).

Furthermore, in order to get the correct concentration in the cell culture plate the two compounds were preincubated at over 17 times their normal concentrations to make up for dilution. Despite favorable conditions for a chemical interaction, elevated compound concentration and a temperature of 37°C, RBV remained fully functional indicating no chemical alteration occurred to RBV. It may be possible, however, that the interaction between RIC-1 and RBV is occurring much faster than can be measured with these large time scales. In order to measure for a rapid chemical reaction, metabolite analysis using mass spectroscopy would be required to monitor any changes in the structure of RBV due to incubation with RIC compounds.

RIC-1 however did experience a loss in efficacy due to preincubation. The loss of function occurs independent of RBV as RIC-1 incubated alone for 6 hours was completely ineffective against both preincubated and "fresh" RBV (Figure 7b). This instability is most interesting as the RBV treatment period for this and all previous assays occurs over 72 hours suggesting RIC-1 is able to inhibit RBV 66 hours after it should have lost all functionality. The prolonged activity of RIC in cell culture might stem from either an increased stability due to interaction with the cell resulting for instance in aggregation or by a rapid mechanism of action resulting in a long lasting alteration to a necessary cellular factor for the MOA of RBV.

In order to better understand how the RIC series inhibited RBV in a prolonged assay, we

looked at the kinetics of association between RIC-1 and RIC-2 with their target of interaction by incubating the RIC compound with MDCK cells for short periods of time and then thoroughly rinsing away any excess unbound compound. The rinse consisted of four separate volumes of 200 uL cold DPBS with five aspirations and redispensing steps with each volume in order to insure complete removal of any unassociated or weakly bound RIC compound. The thoroughness of the wash was intended to remove any RIC not taken up by the cell. New media treated with 45 uM RBV was added and cells were infected. In this way only the RIC utilized in the short incubation was available to inhibit RBV left in the media for the entire 72 hour infection.

The results from Figure 8 indicate that an incubation of RIC-1 with cells for only 2.5 minutes completely inhibited RBV for the entire assay. Compared to the control dilution in Figure 8a, decreasing the incubation time resulted in a more dramatic decrease in viral growth at the lower concentrations (<0.8 uM RIC-1). In contrast no time dependent effect is seen on the higher concentrations of RIC suggesting a saturation effect. The presence of a saturation point would suggest a rate limiting step either in the uptake of RIC-1 or the utilization of RIC-1 possibly resulting from a limit on the amount of possible intracellular RIC-1, the RIC-1 amount where all cellular target proteins are bound, or it may represent the concentration where a sufficient amount of RIC is stored in the cell for later use. The maximum concentration at which RIC-1 can be fully utilized by the cell is 0.8 uM RIC for 2.5 minutes. Decreasing the incubation time or RIC-1 concentration below this saturation point seems to result in an insufficient amount of RIC-1 acquired by the cell. Interestingly, RIC-2 appears to have a higher saturation point of 3.0 uM RIC-2

for 60 minutes, suggesting a mechanism not purely based on diffusion to the cell. If the rate limiting step were based solely on the rate of diffusion of RIC into the cell then the two compounds should have an equal minimum concentration/time. Our assumption is that the structural similarity between the two compounds results in their use of the same transport protein into the cell. These data indicate that a common protein between the two compounds binds RIC-1 more efficiently than RIC-2. Two possible explanations could be RIC-1 is more efficiently transported into the cell, or RIC-1 has a greater affinity for its target site and is able to bind with a greater frequency than RIC-2.

Figure 11 further shows that an increase in the concentration of RBV is able to competitively overcome RIC compound inhibition with RIC-2 being overwhelmed at lower concentrations of RBV than RIC-1. These data indicate RIC-1 and RIC-2 may competitively inhibit a protein which otherwise would directly interact with RBV or an intermediate target necessary for RBV activity. The ability to reverse RIC-1 inhibition is suggestive of a long term interaction with its target protein rather than a permanent alteration leading to degradation or inactivity. If the RIC series reversed RBV via a transient protein binding event leading to a chemical alteration of that protein then we would not expect to see a competitive reversal. Figure 11 is better explained by RIC binding to a shared protein with higher affinity which could then be subsequently reversed due to increased RBV concentrations. Taken together these data might indicate RIC quickly binds to a necessary protein in RBV's mechanism of viral inhibition with a stronger affinity thereby preventing binding of RBV. Furthermore, this binding could result in the stabilization of RIC compound enabling a continuous long term inhibition of

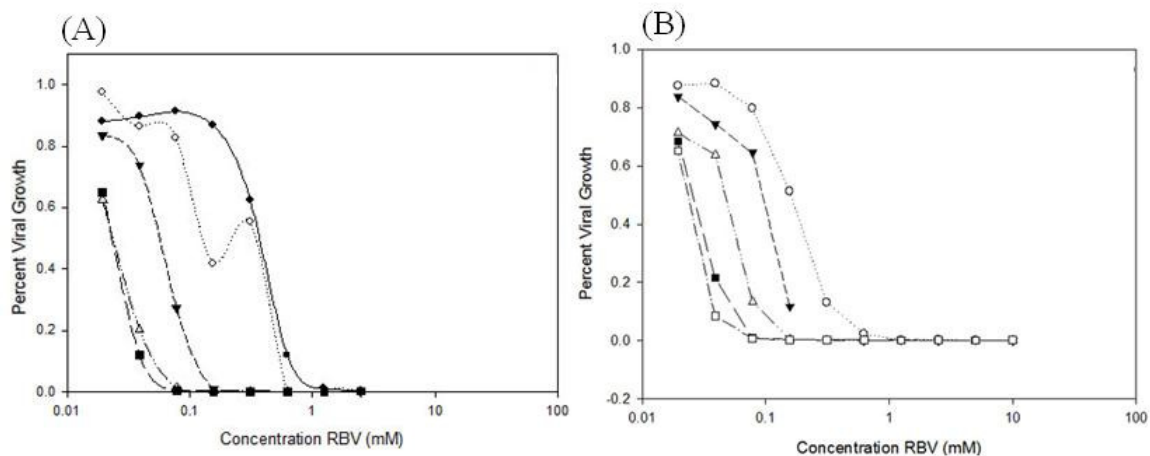


Figure 11: Efficacy of RIC-1 and RIC-2 against increasing RBV concentrations. Panel A. A dilution of RIC-1 (5.64 uM=solid line w/ filled circles, 0.447 uM=dotted line w/open circles, 0.126 uM=dashed line w/filled triangles, 0.010 uM= dashed/dotted line w/ open triangles, and 0.0 uM RIC-1 control= dashed/dotted with filled squares) was incubated with different concentrations of RBV. **B.** The concentrations of RIC-2 used were; 3.942 uM=dotted line w/open circles, 1.323 uM=dashed line w/filled triangles, 0.444 uM= dashed/dotted line w/ open triangles, 0.05 uM= long dashed w/ filled squares, and 0.0 uM RIC-2 control= dashed/dotted with open squares. All data points represent a single replicate. Viral growth was based on neuraminidase activity and compared to virus only controls.

RBV binding.

While binding of RIC prevents RBV binding it does so in a manner without further affecting viral growth. That is, treatment with increasing levels of RIC-1 and RIC-2 did not result in an increase in growth above control levels and only negatively affected viral growth due to cellular cytotoxicity (Figure 11). We further verified this by treating a viral infection with only RIC-1 and RIC-2 in the absence of RBV. No dose dependent variation was seen due to treatment (data not shown). Furthermore, each viral growth assay contained a RIC only dilution control to insure no variation in growth resulted from the compound alone. RIC may interact via an allosteric site or through a unique interaction separate from the RBV/protein interaction.

We began further investigation with the first protein RBV comes in contact with, the equilibrative nucleoside transporter. All RBV uptake into the cell is mediated by the ENT-1 and ENT-2 nucleoside transporters. A possible interaction between ENT-1 and the RIC

series was investigated by measuring the amount of intracellular RBV in the presence of RIC. While the exact mechanism of RBV viral inhibition is unclear there is a general consensus that RBV must first be transported into the cell prior to functionality. Inhibition of ENT-1 and subsequent RBV uptake would thereby prevent its viral inhibition. Furthermore if RIC bound to ENT-1 in such a way to block RBV transport, increasing RBV concentration theoretically could competitively alleviate the blockage explaining the competitiveness seen in Figure 11. Unfortunately, due to the positive control's (NBMPR) inability to alter RBV levels, ENT-1 involvement is still unclear. However, it is our belief that the failure of NBMPR to decrease measured RBV stems from a failure of the compound itself rather than the experimental setup. In order to judge the efficacy of NBMPR in inhibiting RBV we cotreated a plate with dilutions of NBMPR (0.01 uM up to 10 uM) at different RBV concentrations (0.01 uM up to 5 mM). Viral growth remained inhibited at all combinations of the dilutions. NBMPR did not demonstrate a dose dependent or even minor increase in viral growth even at nanomolar concentrations of RBV. Previous RBV uptake studies show an effective inhibition of RBV uptake by ENT-1 at 10 uM NBMPR against 5 uM RBV [41,42,44,45]. Complete inactivity in both the viral readout and uptake assays would suggest an inactive stock solution of NBMPR. Furthermore, the mass spectrometry readout of the 1x, 5x and 10x samples maintained a dose dependent final concentration of RBV with little variation between replicates suggesting an accurate measure of the RBV per well.

However, with the failure of the positive control we can only speculate as to the location of the RBV being measured, whether it is intracellular, extracellular (bound to the plate or

residual) RBV left by the wash, or if the RBV was bound to the cellular membrane. The tight standard deviations between replicates could suggest against residual RBV left behind by the wash, as we would expect a greater variation between replicates if this were the case. The low standard deviation for all samples must stem from a consistent retention of RBV. Unfortunately a longer more thorough wash with the intent of removing any trace RBV and excluding the residual RBV hypothesis would result in an equilibration of RBV out of the cell (Figure 9). Since a longer wash could result in less extra and less intracellular RBV this technique does not help to clarify the origin of the measured RBV. Concerning membrane bound RBV, the procedures used for treatment of cells, rinsing, and collection of the monolayer were similar to those used by other groups [41,42,45]. No mention of trans-membrane RBV binding was reported as a source of error by these groups.

The possibility of failure of the positive control due to a breakdown of the NBMPR compound allows room for further speculation concerning interpretation of Figure 9. While these results are at this point purely speculative equal concentrations of RBV were seen in the RBV only plate and the one pretreated with RIC-1. Since we have shown RIC-1 to be functional in returning viral growth to control levels with a viral readout, with ENT-1 inhibition we would expect to produce a variation in the RBV concentration. As a variation does not exist despite a functional RIC-1 compound these results may be suggestive of an MOA independent of ENT-1. Repeating this uptake experiment with a new ENT-1 inhibitor and or a new functional NBMPR stock would conclusively determine the validity of these speculations. If however NBMPR was in fact functional

these data would indicate a failure of the experiment to accurately measure the internal RBV levels as treatment with NBMMPR should result in a dramatic increase in internalized RBV. This is not shown by the data.

Finally, the role of the IMPDH pathway in RBV inhibition was investigated by measuring the effect of RIC-1 on IMPDH inhibition by Mycophenolic Acid. Ribavirin has been shown to act as an inhibitor of IMP dehydrogenase thereby preventing de novo purine nucleotide synthesis [47]. Inhibiting the conversion of IMP to XMP causes an imbalance in the cellular nucleotide pool which is then responsible for the increased mutation rate and decline in viral growth [47,48,49]. We found that decreased viral growth as a result of IMPDH inhibition with the inhibitor MPA did not respond to treatment with RIC-1 (Figure 10a). The identical increase seen at 15uM RIC-1 for all concentrations of MPA tested is attributed to the cytotoxicity of RIC-1 at that concentration (Figure 1b). Decreasing the cellular fitness and metabolic rate would leave it more vulnerable to viral infection. The reduction in the number of nucleotides used by the host leaves a larger available stock for the viral polymerase resulting in an increased burst size explaining the sudden increase at this concentration. Alternatively the data could suggest a threshold value necessary for activity against MPA. If this were the case however we would expect to see a larger increase in viral growth at the smaller dilutions of MPA. Since all concentrations are affected in a similar manner the effect is concluded to be dependent on the RIC-1 concentration's cytotoxicity.

There are two types of IMPDH inhibitor, both of which have been shown to result in antineoplastic, antiviral and immunosuppressive activity. Nucleoside inhibitors such as

RBV are typically nucleoside analogs while non-nucleoside inhibitors mimic co-factors of IMPDH such as NAD [49]. MPA acts as a non-nucleoside IMPDH inhibitor and therefore acts in a unique pathway separate from RBV. For this reason RIC-1's inactivity against MPA cannot be correlated directly to RBV. We have shown that if RIC-1 were a competitive inhibitor of RBV binding to IMP dehydrogenase it does so without affecting non-nucleoside inhibition. Future research would investigate a possible interaction of RIC-1 in preventing the inhibition of the IMPDH pathway with the nucleoside inhibitor tiazofurin. This would more accurately correlate to a RBV specific MOA.

While the intended function of the RIC series was eliminated, this compound series demonstrates competitive inhibition of a necessary protein in RBV's MOA. Further research into ENT-1 and IMPDH inhibition may further clarify a currently unclear antiviral mechanism resulting from treatment with RBV. If RIC-1 is shown to alleviate inhibition of IMPDH by a different nucleoside inhibitor this data would be among the first to identify RBV's antiviral mechanism of action as being dependent on inhibition of the IMPDH pathway in influenza.

References

1. **Lauring AS, Andino R.** 2010. Quasispecies Theory and the Behavior of RNA Viruses. *PLoS Pathog.* **6**(7): e1001005. doi:10.1371/journal.ppat.1001005
2. **Beigel JH, Farrar J, Han AM, Hayden FG, Hyer R, et al.** 2005. Avian influenza A (H5N1) infection in humans. *N Engl J Med* **353**: 1374–1385.
3. **Dawood FS, Jain S, Finelli L, Shaw MW, Lindstrom S, et al.** 2009 Emergence of a novel swine-origin influenza A (H1N1) virus in humans. *N Engl J Med* **360**:2605–2615.
4. **Rambaut A, Posada D, Crandall KA, Holmes EC.** 2004. The causes and consequences of HIV evolution. *Nat Rev Genet* **5**: 52–61.
5. **Duffy, S., L. A. Shackelton, and E. C. Holmes.** 2008. Rates of evolutionary change in viruses: patterns and determinants. *Nat. Rev. Genet.* **9**:267–276.
6. **Arbiza et al.** 2010. Viral quasispecies profiles as the result of the interplay of competition and cooperation. *BMC Evolutionary Biology* 2010, **10**:137
7. **Batschelet, E., E. Domingo, and C. Weissmann.** 1976. The proportion of revertant and mutant phage in a growing population, as a function of mutation and growth rate. *Gene* **1**:27–32
8. **Drake, J. W., and J. J. Holland.** 1999. Mutation rates among RNA viruses. *Proc. Natl. Acad. Sci. U. S. A.* **96**:13910–13913
9. **Steinhauer, D. A., J. C. de la Torre, E. Meier, and J. J. Holland.** 1989. Extreme heterogeneity in populations of vesicular stomatitis virus. *J. Virol.* **63**:2072–2080.
10. **Eigen M.** 1971. Self-organization of matter and the evolution of biological macromolecules. *Naturwissenschaften* **58**: 465–523
11. **Domingo E, Martin V, Perales C, Grande-Perez A, Garcia-Arriaza J, et al.** 2006. Viruses as quasispecies: biological implications. *Curr Top Microbiol Immunol* **299**: 51–82
12. **Domingo E, Sabo D, Taniguchi T, Weissmann C.** 1978. Nucleotide sequence heterogeneity of an RNA phage population. *Cell* **13**: 735–744.
13. **Hoffman, Randy, Natalie Betz, and Michael Bjerke.** 2001. Shine a Brighter Light on Cell Viability. Promega Corporation, Web. <http://www.promega.com/resources/articles/pubhub/promega-notes-2001/celltiter-glo-assay-flexible-luminescent-cell-viability-assay>
14. **Lauring AS, Andino R.** 2011. Exploring the Fitness Landscape of an RNA Virus by Using a Universal Barcode Microarray. *J Virol.* **85**: 3780-3791
15. **Pfeiffer, J. K., and K. Kirkegaard.** 2005. Increased fidelity reduces poliovirus fitness and virulence under selective pressure in mice. *PLoS Pathog.* **1**:e11.
16. **Sanz-Ramos, M., F. Diaz-San Segundo, C. Escarmis, E. Domingo, and N. Sevilla.** 2008. Hidden virulence determinants in a viral quasispecies in vivo. *J. Virol.* **82**:10465–10476.
17. **Vignuzzi, M., J. K. Stone, J. J. Arnold, C. E. Cameron, and R. Andino.** 2006. Quasispecies diversity determines pathogenesis through cooperative interactions in a viral population. *Nature* **439**:344–348.
18. **Biebricher CK, Eigen M.** 2005. The error threshold. *Virus Res* **107**: 117–127
19. **Eigen M.** 2002. Error catastrophe and antiviral strategy. *Proc Natl Acad Sci USA* **99**: 13374–13376.
20. **Malim MH.** 2009. APOBEC proteins and intrinsic resistance to HIV-1 infection. *Philos Trans R Soc Lond, B, Biol Sci* **364**: 675–687.
21. **Anderson JP, Daifuku R, Loeb LA.** 2004. Viral error catastrophe by mutagenic nucleosides. *Annu Rev Microbiol* **58**: 183–205
22. **Crotty S, Cameron CE, Andino R.** 2001. RNA virus error catastrophe: direct molecular test by using ribavirin. *Proc Natl Acad Sci U S A* **98**: 6895–6900.
23. **Crotty S, Maag D, Arnold JJ, Zhong W, Lau JY, et al.** 2000. The broadspectrum antiviral ribonucleoside ribavirin is an RNA virus mutagen. *Nat Med* **6**: 1375–1379.
24. **Severson WE, Schmaljohn CS, Javadian A, Jonsson CB.** 2003. Ribavirin causes error catastrophe during Hantaan virus replication. *J Virol* **77**: 481–488.
25. **Arnold JJ, Vignuzzi M, Stone JK, Andino R, Cameron CE.** 2005 Remote site control of an active

- site fidelity checkpoint in a viral RNA-dependent RNA polymerase. *J Biol Chem* **280**: 25706–25716.
26. **Pfeiffer JK, Kirkegaard K.** 2003. A single mutation in poliovirus RNA dependent RNA polymerase confers resistance to mutagenic nucleotide analogs via increased fidelity. *Proc Natl Acad Sci U S A* **100**: 7289–7294.
 27. **Vignuzzi M, Stone JK, Arnold JJ, Cameron CE, Andino R.** 2006. Quasispecies diversity determines pathogenesis through cooperative interactions in a viral population. *Nature* **439**: 344–348.
 28. **Bougie, I., and M. Bisailon.** 2003. Initial binding of the broad spectrum antiviral nucleoside ribavirin to the hepatitis C virus RNA polymerase. *J. Biol. Chem.* **278**:52471–52478.
 29. **Dixit, N. M., and A. S. Perelson.** 2006. The metabolism, pharmacokinetics and mechanisms of antiviral activity of ribavirin against hepatitis C virus. *Cell. Mol. Life Sci.* **63**:832–842.
 30. **Maag, D., C. Castro, Z. Hong, and C. E. Cameron.** 2001. Hepatitis C virus RNA-dependent RNA polymerase (NS5B) as a mediator of the antiviral activity of ribavirin. *J. Biol. Chem.* **276**:46094–46098.
 31. **Vo, N. V., K. C. Young, and M. M. Lai.** 2003. Mutagenic and inhibitory effects 4546 IBARRA AND PFEIFFER J. VIROL. of ribavirin on hepatitis C virus RNA polymerase. *Biochemistry* **42**:10462–10471.
 32. **Crotty, S., C. E. Cameron, and R. Andino.** 2001. RNA virus error catastrophe: direct molecular test by using ribavirin. *Proc. Natl. Acad. Sci. USA* **98**:6895–6900.
 33. **Crotty, S., D. Maag, J. J. Arnold, W. Zhong, J. Y. Lau, Z. Hong, R. Andino, and C. E. Cameron.** 2000. The broad-spectrum antiviral ribonucleoside ribavirin is an RNA virus mutagen. *Nat. Med.* **6**:1375–1379.
 34. **Vignuzzi, M., J. K. Stone, and R. Andino.** 2005. Ribavirin and lethal mutagenesis of poliovirus: molecular mechanisms, resistance and biological implications. *Virus Res.* **107**:173–181
 35. **Bougie, I., and M. Bisailon.** 2003. Initial binding of the broad spectrum antiviral nucleoside ribavirin to the hepatitis C virus RNA polymerase. *J. Biol. Chem.* **278**:52471–52478.
 36. **Maag, D., C. Castro, Z. Hong, and C. E. Cameron.** 2001. Hepatitis C virus RNA-dependent RNA polymerase (NS5B) as a mediator of the antiviral activity of ribavirin. *J. Biol. Chem.* **276**:46094–46098.
 37. **Vo, N. V., K. C. Young, and M. M. Lai.** 2003. Mutagenic and inhibitory effects 4546 IBARRA AND PFEIFFER J. VIROL. of ribavirin on hepatitis C virus RNA polymerase. *Biochemistry* **42**:10462–10471.
 38. **Lowe, J. K., L. Brox, and J. F. Henderson.** 1977. Consequences of inhibition of guanine nucleotide synthesis by mycophenolic acid and virazole. *Cancer Res.* **37**:736–743.
 39. **Muller, W. E., A. Maidhof, H. Taschner, and R. K. Zahn.** 1977. Virazole (1--D-ribofuranosyl-1,2,4-triazole-3-carboxamide; a cytostatic agent. *Biochem. Pharmacol.* **26**:1071–1075.
 40. **Sintchak, M. D., and E. Nimmegern.** 2000. The structure of inosine 5-monophosphate dehydrogenase and the design of novel inhibitors. *Immunopharmacology* **47**:163–184.
 41. **Ibarra, K. D., and J. K. Pfeiffer.** 2009. Reduced Ribavirin Antiviral Efficacy via Nucleoside Transporter-Mediated Drug Resistance. *Journal of Virology* **83**:9: 4538-547.
 42. **Fotoohi, A. K., M. Lindqvist, C. Peterson, and F. Albertioni.** 2006. Involvement of the concentrative nucleoside transporter 3 and equilibrative nucleoside transporter 2 in the resistance of T-lymphoblastic cell lines to thiopurines. *Biochem. Biophys. Res. Commun.* 343208-215.
 43. **Gerrish PJ, Garcia-Lerma JG.** 2003. Mutation rate and the efficacy of antimicrobial drug treatment. *Lancet Infect Dis* **3**: 28–32.
 44. **Steinhauer DA, Holland JJ.** 1987. Rapid evolution of RNA viruses. *Annu Rev Microbiol* **41**: 409–433.
 45. **Ibarra, K. D., Jain MK and J. K. Pfeiffer.** 2011. Host-based ribavirin resistance influences hepatitis C virus replication and treatment response. *J Virol.* **85**: 7273-83
 46. **Endres CJ, Moss AM, Ke B, Govindarajan R, Choi DS, et al.** 2009. The role of the equilibrative nucleoside transporter 1 (ENT1) in transport and metabolism of ribavirin by human and wild-type or Ent1-/- mouse erythrocytes. *J Pharmacol Exp Ther.* **329**:387–398.

47. **Lieven J Stuyver***, **Stefania Lostia**, **Steven E Patterson**, **Jeremy L Clark**, **Kyoichi A Watanabe**, **Michael J Otto** and **Krzysztof W Pankiewicz**. 2003. Inhibitors of the IMPDH enzyme as potential antiovine viral diarrhoea virus agents. *Antiviral Chemistry & Chemotherapy* **13**:345–352
48. **Lau JY**, **Tam RC**, **Liang TJ** & **Hong Z**. 2002. Mechanism of action of ribavirin in the combination treatment of chronic HCV infection. *Hepatology* **35**:1002–1009.
49. **Franchetti P** and **Grifantini M**. 1999. Nucleoside and non-nucleoside IMP dehydrogenase inhibitors as antitumor and antiviral agents. *Current medicinal chemistry* **6**:7:599-614
50. **Iikura M.**, **Furihata T.**, **Mizuguchi M.**, **Nagai M.**, **Ikeda M.**, **Kato N.**, **Tsubota A.**, and **Chiba K**. 2012. ENT1, a Ribavirin Transporter, Plays a Pivotal Role in Antiviral Efficacy of Ribavirin in a Hepatitis C Virus Replication Cell System. **56**:1407-1413
51. **Sleigh M.J.**, **Both G.W.**, **Brownless G.G**. 1979 A new method for the size estimation of the RNA genome segments of influenza virus. *Nucleic Acids Research*. **6**: 1309-1321

Cell image taken from <http://cronodon.com/BioTech/Cells.html>

Translation image taken from http://www.mun.ca/biology/scarr/iGen3_05-01.html

hENT1 <http://www.clavispharma.com/technology/biomarkers-hent1>

IMPDH <http://www.nature.com/nchembio/journal/v7/n12/full/nchembio.693.html>